Revista Mexicana de Astronomía y Astrofísica, **49**, 333–343 (2013)

TIME VARIATION OF THE O/H RADIAL GRADIENT IN THE GALACTIC DISK BASED ON PLANETARY NEBULAE

W. J. Maciel and R. D. D. Costa

Instituto de Astronomia, Geofísica e Ciências Atmosféricas
Universidade de São Paulo, Brazil

Received 2013 May 31; accepted 2013 August 8

RESUMEN

La controversia sobre la variación en el tiempo de los gradientes radiales de abundancias puede, en principio, ser resuelta estimando los gradientes a partir de nebulosas planetarias (PN) que provengan de estrellas centrales (CSPN) de distintas edades. En este trabajo consideramos cuatro muestras de CSPN cuyas edades han sido estimadas por tres métodos distintos, y estimamos los gradientes de la abundancia de oxígeno para estos objetos. Los resultados sugieren pequeñas diferencias entre las CSPN más jóvenes y las más viejas. Los objetos más jóvenes tienen abundancias de oxígeno similares o un poco mayores que las de los objetos más viejos, y los gradientes son similaares para ambos grupos. En consecuencia, el gradiente radial de O/H no ha cambiado apreciablemente durante los tiempos de vida de los objetos estudiados, de modo que no se espera que los gradientes para las PN sean muy distintos de los observados en objetos más jóvenes, lo cual parece encontrar sustento en datos observacionales recientes.

ABSTRACT

The controversy on the time variation of the radial abundance gradients can in principle be settled by estimating the gradients from planetary nebulae (PN) ejected by central stars (CSPN) with different ages. In this work, we consider four samples of CSPN whose lifetimes have been estimated using three different methods and estimate the oxygen abundance gradients for these objects. The results suggest some small differences between the younger and older CSPN. The younger objects have similar or slightly higher oxygen abundances compared with the older objects, and the gradients of both groups are similar within the uncertainties. Therefore, the O/H radial gradient has not changed appreciably during the lifetime of the objects considered, so that PN gradients are not expected to be very different from the gradients observed in younger objects, which seems to be supported by recent observational data.

Key Words: Galaxy: abundances — Galaxy: Disk — ISM: abundances — planetary nebulae: general

1. INTRODUCTION

Radial abundance gradients are observed in the galactic disk based on abundance measurements of several chemical elements in a variaty of astronomical objects (Henry & Worthey 1999; Maciel & Costa 2010; Maciel, Rodrigues, & Costa 2012). The main chemical elements are oxygen, neon, sulphur and argon in photoionized nebulae, and iron in stars. However, recent work also includes data on many other elements, especially in Cepheids, such as Ba (Andrievsky et al. 2013), several α-elements, iron-peak elements, and even heavier elements (see for example Cescutti et al. 2007). In view of the variety of chemical elements and objects, the gradients are especially important as constraints of chemical evolution models, which is stressed by the fact that the gradients do not appear to be constant, but present both space and time variations, which increases the number of constraints that must be satisfied by realistic models.

The problem of the time variation of the abundance gradients –here understood as the *slope* of the gradients, usually measured in dex kpc^{-1}– is particularly important, as it is instrumental in distinguishing between different chemical evolution models. For example, the model by Chiappini, Matteucci, & Romano (2001) predicts a continuous steepening of the gradients with time, while models by Hou, Prantzos, & Boissier (2000) predict just the opposite behavior. Estimating the gradients at different epochs is a difficult problem, as it implies some knowledge of the ages of the objects involved, apart from their chemical abundances and distances. As is well known, stellar ages are uncertain, especially considering evolved objects, with ages greater than about 2 to 3 Gyr (see for example Soderblom 2009, 2010).

While the present day gradient may be determined on the basis of the observed abundances of young objects, such as HII regions, with typical ages of a few million years, or cepheid variables, with ages up to a few hundred million years (see for example Maciel, Lago, & Costa 2005), the gradient at past epochs is more appropriately studied on the basis of planetary nebulae (PN) and open clusters. PN are formed by progenitor stars with masses in the approximate range of 0.8 to 8 $M_{\odot}$ on the main sequence, so that their ages would be expected to vary from about 1 Gyr to several Gyr, as indicated for example by Table 7 of Stasińska (2004). On the other hand, open clusters have an even broader time range from a few million years up to several Gyr (see for example Andreuzzi et al. 2011 or the most recent version of the open cluster catalogue by Dias et al. 2002).

In a previous work (Maciel, Costa, & Uchida 2003), we studied the time variation of the abundance gradients using planetary nebulae based largely on their classification according to the Peimbert scheme (Peimbert 1978). While this scheme succeeds in predicting average ages and central star masses (see for example Stasińska 2004, Table 7), the derived results are of difficult interpretation, since the adopted classification implies some ambiguity in the stellar properties for many objects.

In order to improve this investigation, we have developed five methods to estimate individual ages of CSPN, as opposed to the average ages implied by the Peimbert types. These methods are based either on the measured nebular abundances or on the kinematic properties of the nebulae and their central stars. In the first paper (Maciel, Costa, & Idiart 2010), we developed three methods based on the chemical abundances, using (1) an age-metallicity-distance relation, (2) a simpler age-metallicity relation, and (3) a relation between the central star masses and the nebular nitrogen abundances (see also Maciel et al. 2003, 2005). More recently (Maciel, Rodrigues, & Costa 2011), we developed two kinematic methods based on the velocity dispersion-age relation from the Geneva-Copenhagen survey (Holmberg, Nordström, & Andersen 2009) using (4) the galactic rotation curve or (5) the U, V, W velocity components.

The five methods 1–5 above were applied to different samples of galactic PN with known properties, and the age distributions were determined in each case. Based on these results, most CSPN in the galactic disk have ages under 6 Gyr, and the age distribution has a prominent peak, but its exact location depends on the adopted method. In the present work, we selected the most accurate of the five methods developed so far, namely Methods 1, 3, and 5, and applied them to different samples of galactic PN in order to investigate the time variation of the radial abundance gradients. Method 2 fails to produce a prominent peak in contrast with the most reliable methods, and Method 4 depends on several assumptions regarding the actual PN rotation curve, so that these methods are not included in the present work. In § 2 we summarize the main characteristics of the methods considered in this investigation and in § 3 we describe the PN samples adopted. In § 4 we describe the procedure used to estimate the gradients at different times and the main results are presented and discussed, and in § 5 the main conclusions are stated.

2. AGE DETERMINATION OF CSPN

2.1. *Method 1: The Age-metallicity-radius relation*

Method 1 was discussed in detail by Maciel et al. (2003), where it was also called Method 1, and it was applied to a sample of planetary nebulae in the galactic disk by Maciel et al. (2010). It uses a relationship between the ages of the PN progenitor stars, the nebular abundances, and the galactocentric distances developed by Edvardsson et al. (1993). The original relation involves the [Fe/H] metallicities, which are obtained from the oxygen abundances measured in the nebulae using a relation developed by Maciel et al. (2003). The age distribution obtained for the original sample of 234 nebulae by Maciel et al. (2010) is shown in Figure 1. It can be seen that a well-defined peak exists in the age distribution at about 4–5 Gyr.

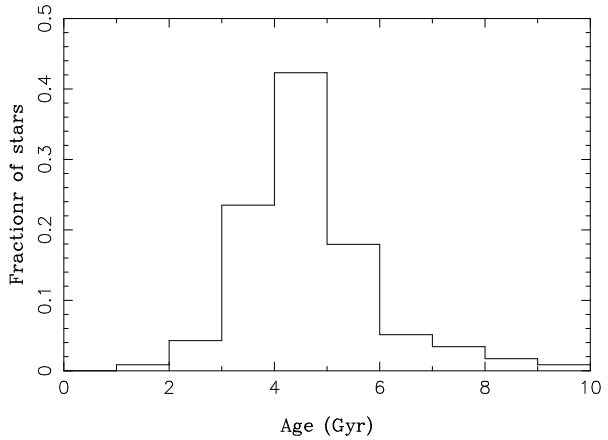

Fig. 1. Age distribution of the central stars of planetary nebulae for Method 1, based on an age-metallicity-galactocentric distance relation.

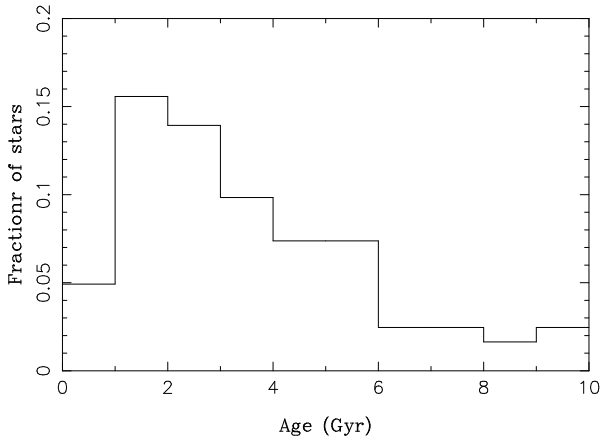

Fig. 2. Age distribution of the central stars of planetary nebulae for Method 3, based on an relation between the central star mass and the nebular N/O ratio.

2.2. *Method 3: The N/O × CSPN mass relation*

Method 3 is based on a relationship between the mass of the planetary nebula central star and the N/O abundance ratio measured in the nebulae also developed by Maciel et al. (2003), and based on an earlier analysis of a selected sample of galactic nebulae (Cazetta & Maciel 2000). The method also assumes an initial mass-final mass relation for the central stars, and we adopt here Case B of Maciel et al. (2010), which uses the mass-age relation by Bahcall & Piran (1983), and was considered the most realistic case compared with their Case A, which assumes a much simpler mass-age relation leading to very large lifetimes for the more massive stars.

Figure 2 shows the derived age distribution for this method as applied by Maciel et al. (2010) to a sample of 122 galactic nebulae. The distribution is similar to the previous case in the sense that most objects have ages lower than about 6 Gyr, and there is a prominent peak, but the average ages are lower than in the case of Method 1, which reflects the fact that in Method 3 the lifetimes of the massive stars are lower and the probability of finding stars at larger lifetimes is smaller.

2.3. *Method 5: The U,V,W, velocity components*

Method 5 corresponds to Method 2 of Maciel et al. (2011) and it is a kinematic method, in which we have determined the U, V, W velocity components and the total velocity T, as well as the velocity dispersions σ_U, σ_V, σ_W, and σ_T. Accurate relations between the velocity dispersions and the stellar ages were obtained by the Geneva-Copenhagen Survey of the Solar Neighbourhood (cf. Nordström et al. 2004; Holmberg et al. 2007, 2009), which allowed the determination of the ages of the CSPN in our sample.

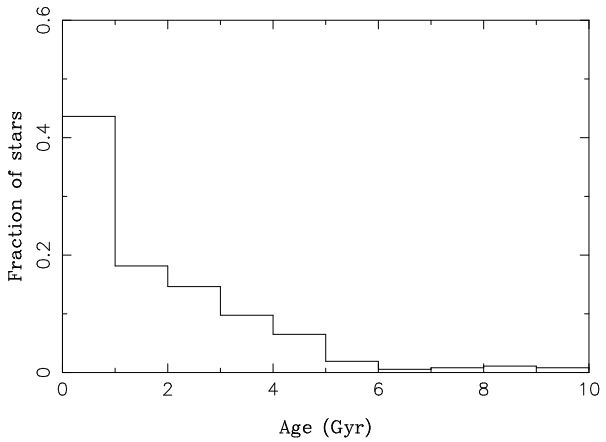

Fig. 3. Age distribution of the central stars of planetary nebulae for Method 5, based on the stellar velocities and on a relation between the velocity dispersion and the stellar age.

Figure 3 shows the age distribution for Method 5 applied to a large sample of planetary nebulae with measured radial velocities from the catalogue by Durand, Acker, & Zijlstra (1998) which contains 867 objects. In this case we have adopted the total T velocities, and distances from the distance scale by Stanghellini, Shaw, & Villaver (2008, hereafter SSV), which are available for 403 objects in the catalogue of Durand et al. (1998). Again, the distribution shows a prominent peak, although it is somewhat displaced towards lower ages compared to the distributions shown in the previous figures.

3. THE PN SAMPLES

We have considered 4 different and independent samples of galacic planetary nebulae, hereafter named Samples A, B, C, and D.

3.1. *Samples A, B, and C*

Sample A is the same sample used by Maciel et al. (2003, 2005), which includes 234 well-observed nebulae in the solar neighbourhood and in the galactic disk. These objects have galactocentric distances in the range $4 < R(\mathrm{kpc}) < 14$. The galactocentric distances R are calculated from the heliocentric distances and the galactic coordinates in a straightforward way for a given value of the solar galactocentric distance, which is usually adopted as $R_0 = 8.0 - 8.5$ kpc. The real uncertainty comes naturally from the heliocentric distances, so that we have adopted two different PN distance scales, as discussed below. Sample B is a smaller sample containing 122 PN with sufficient data for Method 3 as used by Maciel et al. (2003). Sample C is the largest of the two samples used by Maciel et al. (2011) for their Method 2, which corresponds to Method 5 of the present paper. This sample contains all nebulae with accurate radial velocities from the catalogue by Durand et al. (1998). We have adopted the distances by SSV, which reduces the sample to 403 objects. Taking into account only those objects with accurate oxygen abundances, kinematic ages in the interval $0 < t(\mathrm{Gyr}) < 14$ and galactocentric distances in the range $3 < R(\mathrm{kpc}) < 12$, we have a final sample of 168 nebulae. The last restriction is important as the gradient apparently flattens out for $R < 3$ kpc and probably also for $R > 12$ kpc, so that we will be able to estimate the *average* disk gradient at any given epoch.

3.2. *Sample D*

Henry et al. (2010) obtained a sample containing 124 planetary nebulae with homogeneously determined chemical abundances, which in principle allows the determination of more accurate gradients. These objects are located in the galactic disk, so that they are adequate to investigate the presence of radial abundance gradients. In their analysis, Henry et al. (2010) derived an average gradient of -0.058 ± 0.006 dex kpc^{-1} for the O/H ratio, accounting for uncertainties both in the oxygen abundances and in the radial distances, and using a detailed statistical procedure. The homogeneity of the sample derives from the fact that all objects have been observed and analyzed by the same group, using the same observational and reduction techniques (see also Henry, Kwitter, & Balick 2004; Milingo et al. 2010). The adopted distances come largely from the same source in the literature, namely the work by Cahn, Kaler, & Stanghellini (1992, hereafter CKS), and the solar galactocentric distance was taken as 8.5 kpc. Considering the more recent SSV distance scale by Stanghellini et al. (2008), which includes data for 101 objects of the sample, Henry et al. (2010) obtained a somewhat flatter gradient of -0.042 ± 0.004 dex kpc^{-1}.

We have used the sample by Henry et al. (2010) and calculated the individual ages using Methods 1, 3, and 5 above, with the oxygen abundances given in that paper. The N/O abundances needed for Method 3 were taken from the same group for consistency, as given in Henry et al. (2010), Henry et al. (2004), and Milingo et al. (2010). For the objects not found in these samples we have used data from our own compilations, as given by Maciel et al. (2010) and Quireza, Rocha-Pinto, & Maciel (2007). Most of the objects in this sample have galactocentric distances $R < 15$ kpc, which is particularly interesting, since very few anticentre nebulae with large galactocentric distances have been analyzed so far, and the available results suggest a spatial variation of the gradients which is not fully understood (see discussions by Henry et al. 2010; Costa, Uchida, & Maciel 2004).

4. RESULTS AND DISCUSSION

4.1. *Estimating the time variation of the abundance gradients*

In this work we have used the method initially proposed by Maciel et al. (2005), which consists in separating the planetary nebula samples into two groups according to their ages. An age limit t_L is defined and considered as a free parameter, adopting values in the range $1 \leq t_L \leq 14$ Gyr. Then the average O/H abundances and the magnitude of the radial gradients are estimated as functions of the age limit for each of the methods 1, 3, and 5. By comparing the average gradients of the "younger" group with those of the "older" group, we can in principle detect any systematic differences between the two groups considered. In practice the adopted range of the age limit is shorter than indicated above, since both for very young and very old objects one of the groups becomes very small, so that the results become statistically inaccurate. However, as we will see in the following discussion, with age limits in the range $1 \leq t_L \leq 5$ Gyr in most cases the results show a well defined pattern, which is largely independent of the adopted age limit. The formal uncertainties

TABLE 1

RESULTS FOR THE TOTAL SAMPLES

Sample	Method	N	O/H	d(O/H)/dR	r
A	1	234	8.63 ± 0.26	-0.04 ± 0.01	-0.35
B	3	111	8.73 ± 0.20	-0.08 ± 0.01	-0.68
C	5	168	8.64 ± 0.24	-0.03 ± 0.01	-0.21
D (CKS)	1	124	8.59 ± 0.21	-0.04 ± 0.01	-0.53
D (CKS)	3	119	8.59 ± 0.22	-0.04 ± 0.01	-0.53
D (CKS)	5	91	8.62 ± 0.20	-0.04 ± 0.01	-0.53
D (SSV)	1	101	8.56 ± 0.22	-0.03 ± 0.01	-0.54
D (SSV)	3	97	8.60 ± 0.22	-0.04 ± 0.01	-0.56
D (SSV)	5	88	8.62 ± 0.20	-0.03 ± 0.01	-0.53

TABLE 2

RESULTS FOR SAMPLES A, B, C, METHODS 1, 3, 5 (M1, M3, M5)

		Young Group				Old Group			
Sample	t_L	N	O/H	d(O/H)/dR	r	N	O/H	d(O/H)/dR	r
A, M1	2.5	40	8.65 ± 0.27	$+0.02 \pm 0.02$	$+0.13$	194	8.63 ± 0.26	-0.06 ± 0.01	-0.47
	3.0	46	8.68 ± 0.28	-0.00 ± 0.02	-0.03	188	8.62 ± 0.26	-0.06 ± 0.01	-0.52
	3.5	64	8.74 ± 0.28	-0.03 ± 0.01	-0.26	170	8.59 ± 0.24	-0.07 ± 0.01	-0.57
	4.0	89	8.75 ± 0.25	-0.04 ± 0.01	-0.39	145	8.56 ± 0.24	-0.07 ± 0.01	-0.63
	4.5	137	8.73 ± 0.23	-0.05 ± 0.01	-0.49	97	8.49 ± 0.23	-0.08 ± 0.01	-0.67
	5.0	173	8.71 ± 0.23	-0.05 ± 0.01	-0.50	61	8.43 ± 0.24	-0.09 ± 0.01	-0.74
B, M3	3.5	12	8.95 ± 0.23	-0.09 ± 0.01	-0.98	99	8.70 ± 0.18	-0.08 ± 0.01	-0.73
	4.0	34	8.87 ± 0.18	-0.09 ± 0.01	-0.90	77	8.66 ± 0.17	-0.08 ± 0.01	-0.82
	4.5	76	8.79 ± 0.19	-0.09 ± 0.01	-0.83	35	8.59 ± 0.14	-0.07 ± 0.01	-0.84
	5.0	95	8.75 ± 0.20	-0.09 ± 0.01	-0.80	16	8.57 ± 0.11	-0.07 ± 0.01	-0.79
C, M5	1.0	78	8.67 ± 0.23	-0.02 ± 0.01	-0.19	90	8.62 ± 0.25	-0.03 ± 0.01	-0.22
	1.5	91	8.67 ± 0.22	-0.02 ± 0.01	-0.15	77	8.60 ± 0.25	-0.03 ± 0.01	-0.25
	2.0	99	8.67 ± 0.22	-0.02 ± 0.01	-0.19	69	8.60 ± 0.26	-0.03 ± 0.01	-0.23
	2.5	112	8.66 ± 0.23	-0.02 ± 0.01	-0.18	56	8.60 ± 0.25	-0.03 ± 0.02	-0.24
	3.0	121	8.66 ± 0.23	-0.02 ± 0.01	-0.21	47	8.59 ± 0.26	-0.03 ± 0.02	-0.19
	3.5	127	8.66 ± 0.23	-0.03 ± 0.01	-0.22	41	8.58 ± 0.26	-0.02 ± 0.02	-0.14
	4.0	135	8.66 ± 0.23	-0.03 ± 0.01	-0.22	33	8.58 ± 0.27	-0.02 ± 0.02	-0.17

of the methods adopted here, as estimated by Maciel et al. (2010, 2011) are about 1–2 Gyr.

4.2. *Results for Samples A, B, C, and D*

The main results of this paper are shown in Tables 1–4 and in Figures 4–9. The tables show the complete results, as follows: Table 1 gives the results for the complete samples A, B, C, and D for Methods 1, 3, and 5. The selected sample is shown in Column 1, the method used is given in Column 2, the total number N of objects considered, in Column 3, the average O/H abundances and uncertainties, in Column 4, the derived oxygen gradient slope (dex kpc^{-1}) with uncertainties, in Column 5, and the correlation coefficient r in Column 6. The average abundances in Column 4 are simple averages, calculated irrespective of the galactocentric distances. For sample D we show the results using both the CKS and SSV distance scales. Table 2 shows the results for samples A, B and C considering Methods 1, 3, and 5, referred to as M1, M3, and M5, respectively, taking into account two age groups, so that we have

TABLE 3

RESULTS FOR SAMPLE D, DATA BY HENRY ET AL. (2010), CKS DISTANCES

		Young Group				Old Group			
	t_L	N	O/H	d(O/H)/dR	r	N	O/H	d(O/H)/dR	r
M1	3.0	23	8.60 ± 0.21	-0.07 ± 0.01	-0.88	101	8.58 ± 0.22	-0.06 ± 0.01	-0.66
	3.5	45	8.64 ± 0.19	-0.05 ± 0.01	-0.82	79	8.56 ± 0.22	-0.07 ± 0.01	-0.77
	4.0	78	8.63 ± 0.17	-0.04 ± 0.01	-0.70	46	8.51 ± 0.26	-0.08 ± 0.01	-0.88
	4.5	97	8.63 ± 0.17	-0.04 ± 0.01	-0.66	27	8.43 ± 0.28	-0.08 ± 0.01	-0.94
	5.0	111	8.60 ± 0.21	-0.04 ± 0.01	-0.64	13	8.44 ± 0.21	-0.08 ± 0.01	-0.91
M3	1.0	60	8.53 ± 0.25	-0.04 ± 0.01	-0.59	59	8.64 ± 0.16	-0.02 ± 0.01	-0.43
	1.5	84	8.58 ± 0.23	-0.04 ± 0.01	-0.55	35	8.60 ± 0.17	-0.03 ± 0.01	-0.47
	2.0	96	8.58 ± 0.23	-0.04 ± 0.01	-0.55	23	8.60 ± 0.18	-0.03 ± 0.02	-0.39
	2.5	99	8.58 ± 0.22	-0.04 ± 0.01	-0.54	20	8.61 ± 0.19	-0.05 ± 0.02	-0.52
	3.0	102	8.58 ± 0.22	-0.03 ± 0.01	-0.52	17	8.62 ± 0.20	-0.05 ± 0.02	-0.62
	3.5	105	8.58 ± 0.22	-0.03 ± 0.01	-0.52	14	8.60 ± 0.20	-0.06 ± 0.02	-0.68
M5	1.0	44	8.59 ± 0.21	-0.04 ± 0.01	-0.54	47	8.64 ± 0.19	-0.03 ± 0.01	-0.49
	1.5	53	8.60 ± 0.21	-0.04 ± 0.01	-0.54	38	8.64 ± 0.19	-0.03 ± 0.01	-0.49
	2.0	64	8.61 ± 0.21	-0.03 ± 0.01	-0.50	27	8.64 ± 0.19	-0.04 ± 0.01	-0.60
	2.5	73	8.61 ± 0.21	-0.04 ± 0.01	-0.53	18	8.65 ± 0.16	-0.03 ± 0.02	-0.45
	3.0	75	8.61 ± 0.21	-0.03 ± 0.01	-0.52	16	8.65 ± 0.17	-0.05 ± 0.02	-0.60
	3.5	78	8.61 ± 0.21	-0.03 ± 0.01	-0.52	13	8.65 ± 0.19	-0.07 ± 0.02	-0.64

TABLE 4

RESULTS FOR SAMPLE D, DATA BY HENRY ET AL. (2010), SSV DISTANCES

		Young Group				Old Group			
	t_L	N	O/H	d(O/H)/dR	r	N	O/H	d(O/H)/dR	r
M1	3.0	30	8.54 ± 0.22	-0.04 ± 0.01	-0.74	71	8.57 ± 0.23	-0.05 ± 0.01	-0.67
	3.5	47	8.59 ± 0.20	-0.04 ± 0.01	-0.75	54	8.54 ± 0.24	-0.06 ± 0.01	-0.79
	4.0	68	8.59 ± 0.18	-0.03 ± 0.01	-0.69	33	8.50 ± 0.29	-0.07 ± 0.01	-0.90
	4.5	81	8.58 ± 0.18	-0.03 ± 0.01	-0.60	20	8.49 ± 0.34	-0.08 ± 0.01	-0.93
	5.0	91	8.57 ± 0.22	-0.03 ± 0.01	-0.61	10	8.51 ± 0.25	-0.09 ± 0.01	-0.92
M3	1.0	47	8.55 ± 0.27	-0.04 ± 0.01	-0.62	50	8.65 ± 0.16	-0.02 ± 0.01	-0.41
	1.5	68	8.60 ± 0.24	-0.04 ± 0.01	-0.57	29	8.61 ± 0.18	-0.03 ± 0.01	-0.50
	2.0	78	8.60 ± 0.23	-0.04 ± 0.01	-0.58	19	8.61 ± 0.19	-0.04 ± 0.02	-0.46
	2.5	80	8.60 ± 0.23	-0.04 ± 0.01	-0.57	17	8.60 ± 0.20	-0.05 ± 0.02	-0.56
	3.0	83	8.60 ± 0.23	-0.04 ± 0.01	-0.55	14	8.62 ± 0.21	-0.06 ± 0.02	-0.67
	3.5	85	8.60 ± 0.23	-0.04 ± 0.01	-0.55	12	8.60 ± 0.22	-0.06 ± 0.02	-0.72
M5	1.0	42	8.59 ± 0.21	-0.04 ± 0.01	-0.57	46	8.63 ± 0.19	-0.03 ± 0.01	-0.45
	1.5	51	8.60 ± 0.21	-0.04 ± 0.01	-0.56	37	8.65 ± 0.18	-0.03 ± 0.01	-0.45
	2.0	62	8.61 ± 0.21	-0.04 ± 0.01	-0.53	26	8.66 ± 0.18	-0.03 ± 0.01	-0.56
	2.5	71	8.61 ± 0.21	-0.04 ± 0.01	-0.55	17	8.67 ± 0.14	-0.02 ± 0.02	-0.27
	3.0	73	8.61 ± 0.21	-0.03 ± 0.01	-0.54	15	8.67 ± 0.15	-0.03 ± 0.02	-0.38
	3.5	76	8.61 ± 0.21	-0.03 ± 0.01	-0.54	12	8.68 ± 0.16	-0.05 ± 0.04	-0.38

for each adopted age limit t_L in Gyr (Column 2) the number of objects N in the samples, the average O/H abundances, the derived gradients and correlation coefficients for both the young (Columns 3,

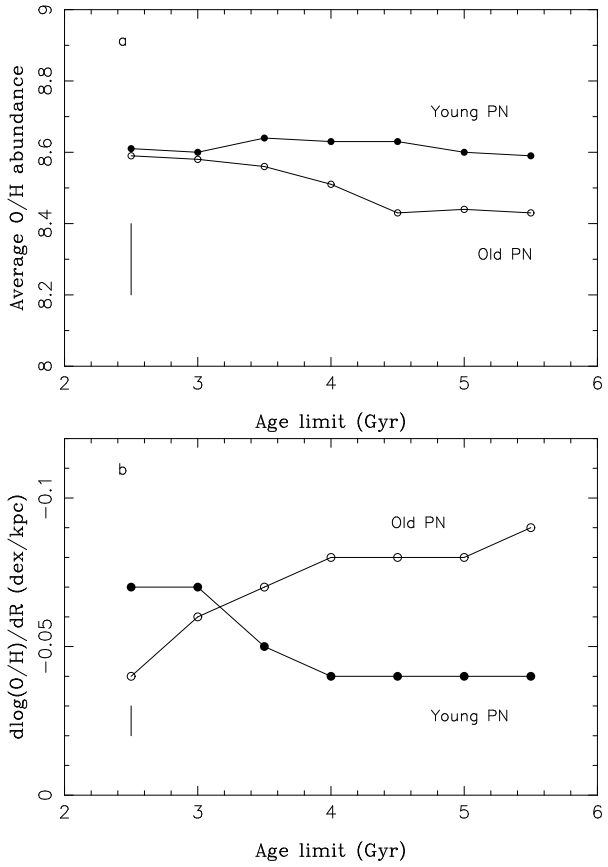

Fig. 4. (a) Average O/H abundances for the young and old groups of PN as a function of the age limit for Method 1, Sample D, data by Henry et al. (2010), and CKS distances). (b) The same for the estimated O/H gradients (dex kpc^{-1}).

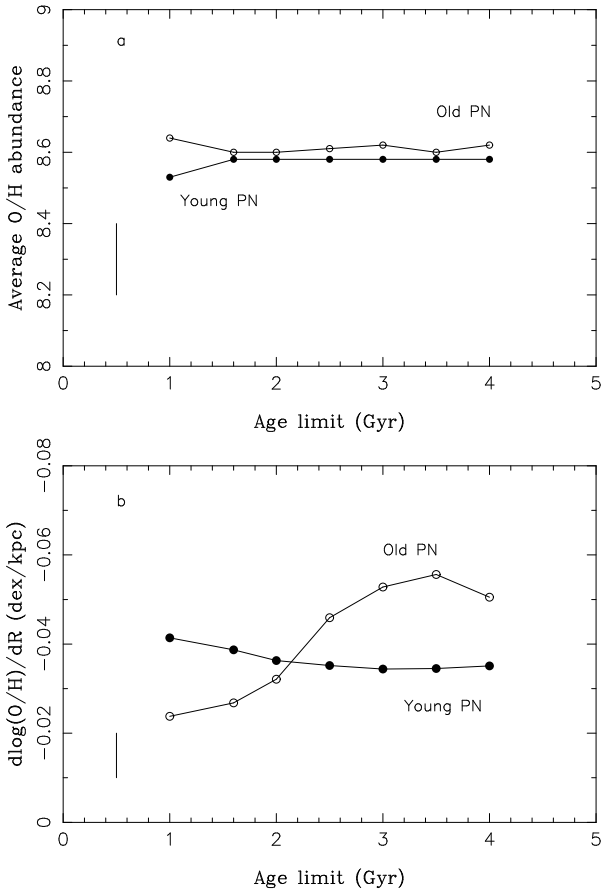

Fig. 5. The same as Figure 4 for Method 3.

4, 5, and 6) and the old (Columns 7, 8, 9, and 10) groups. The corresponding results for Sample D are shown in Tables 3 and 4, for distances by CKS and SSV, respectively. In fact, the results of this paper concerning the average oxygen abundances and the O/H gradients are essentially the same for both the distance scale of Cahn et al. (1992) and that of Stanghellini et al. (2008).

Examples of the procedure adopted here are given in Figures 4, 5, and 6 for Methods 1, 3, and 5, respectively. In these figures, we show the average O/H abundances for the young and old groups as a function of the age limit for Sample D, using data by Henry et al. (2010) with distances by Cahn et al. (1992) (Figures 4a, 5a, and 6a). In Figures 4b, 5b, and 6b we show the corresponding results for the oxygen gradient. In both cases the average uncertainty is shown at bottom left. These figures are representative of all cases studied here, in the sense that there is generally a common pattern in the distribution of the average O/H abundances and the radial gradient with the age limit, which can be observed also in Tables 2, 3, and 4.

Concerning the average abundances, in most cases the younger groups are either systematically more oxygen-rich than the older group or both groups have similar abundances, irrespective of the adopted age limit. The former situation is valid for Samples A, B, and C using Methods 1, 3, and 5, respectively, as shown in Table 2. Also, for Sample D, Tables 3 and 4 and Figure 4 confirm this result for Method 1; for Method 3 the abundances of both groups are similar within the uncertainties, and the reverse is observed for Method 5, although the differences are small. Based on theoretical grounds concerning the chemical evolution of the galactic disk it is expected that the younger groups should be more oxygen-rich, as shown in most cases considered here, in view of the age-metallicity relation observed in the galactic disk. However, the difference is usually small, frequently of the same order of, or even smaller

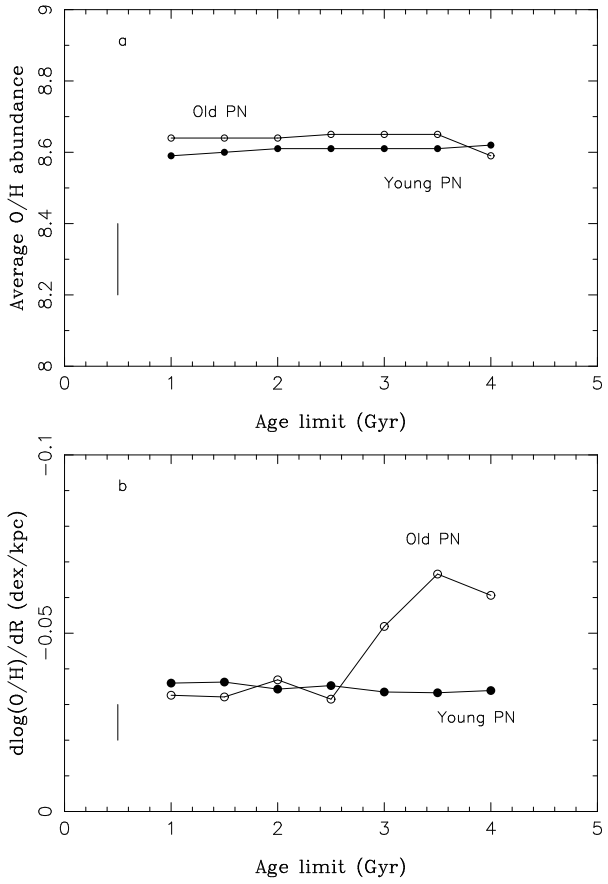

Fig. 6. The same as Figure 4 for Method 5.

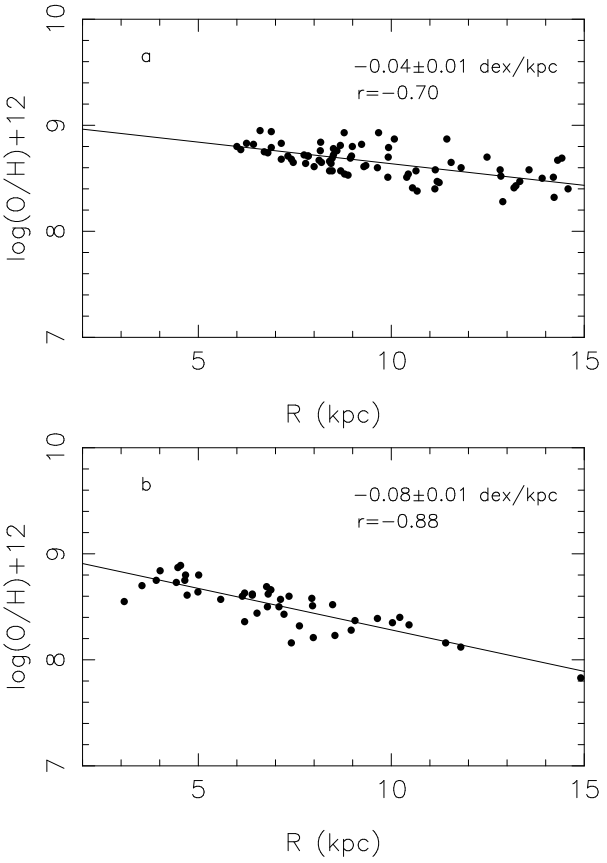

Fig. 7. O/H abundances as a function of the galactocentric distance for Sample D, data by Henry et al. (2010) and CKS distances for Method 1 and age limit 4.0 Gyr. The figures include the slopes (dex kpc^{-1}) and correlation coefficients r. (a) Young group. (b) Old group.

than, the average uncertainty, which can be seen for example in Figures 4 and 5. The inverse behavior observed for Method 5 is probably due to the fact that the ages estimated by this method are generally very small, as can be seen for example in Figure 3, which means that most objects tend to belong to the younger group, thus increasing the average abundances. It should also be mentioned that for the extreme values of the age limit in Tables 2, 3, and 4 one of the samples becomes underpopulated, so that the corresponding results are less reliable. In conclusion, the younger groups have generally slightly higher average abundances compared to the older groups, but the difference in most cases are small, which can be attributed to the well known dispersion in the age-metallicity relation in the Galaxy (Rocha-Pinto et al. 2000, 2006; Feltzing, Holmberg, & Hurley 2001; Bensby, Feltzing, & Lundström 2004; Marsakov et al. 2011).

Considering now the oxygen gradients shown in Tables 2, 3, and 4 and in the examples of Figures 4, 5, and 6, we can observe that in most cases the gradients for both groups are similar within the uncertainties. This is always true for Methods 3 and 5 as applied to all corresponding samples, namely, Samples B, C and D (CKS or SSV). Only for Method 1 we notice that the older group seems to have steeper gradients compared to the younger groups both for Samples A and D, and the difference may reach about 0.03 dex kpc^{-1}, as shown in Figure 4b. Here we may be observing the inverse behavior of the average abundances discussed above, since Method 1 produces preferentially very large ages, so that most of the samples will contain relatively aged objects, which will increase the observed differences between the gradients. A probably more important reason for the differences between the linear gradients calculated by Method 1 is that this method assumes a relation involving the abundances, ages, and galactocentric distances (equation 2 of Maciel et al. 2003). Since the average abundances of both groups do not differ appreciably, this relation implicitly assumes

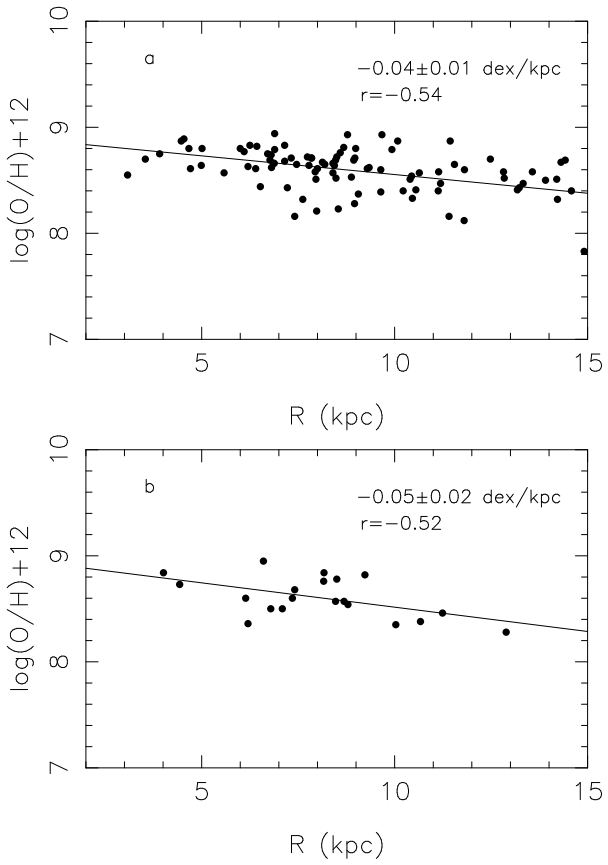

Fig. 8. The same as Figure 7 for Sample D, Method 3, age limit 2.5 Gyr.

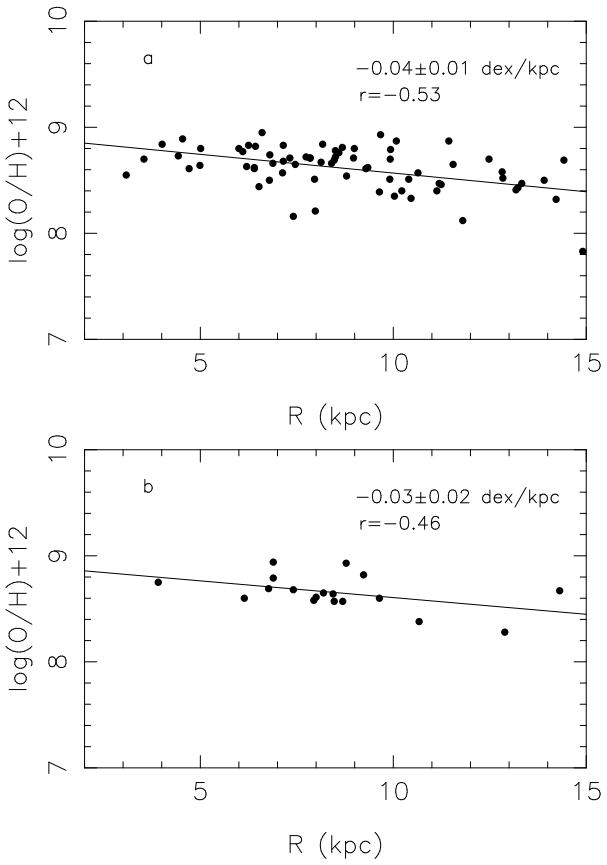

Fig. 9. The same as Figure 7 for Sample D, Method 5, age limit 2.5 Gyr.

that the gradients of the older groups are somewhat steeper than those of the younger groups, which is in fact what is observed in Figure 4b, for example. In all other cases, as exemplified in Figures 5b and 6b, both gradients are similar. In fact, from the discussions on the age determinations given in the previous papers (Maciel et al. 2010, 2011), we would expect Method 1 to be less reliable compared to Methods 3 and 5. Method 5 is in principle more correct, since it is based on more robust correlations between the stellar ages and the kinematic properties, but the hypotheses made in Maciel et al. (2011) concerning the stellar proper motions probably lead to an overestimate of the number of very young objects, which indeed can be observed in Figure 3. Moreover, the age-velocity dispersion relation, as proposed by the Geneva-Copenhagen survey (Holmberg et al. 2009) is less accurate for very young objects, so that we confirm that the results for Method 3, case B, of Maciel et al. (2010) are probably more accurate. The differences between the observed gradients of the young and old groups are shown in the examples of Figures 7–9, where we have considered Sample D by Henry et al. (2010) with distances by CKS. In Figures 7, 8, and 9 the adopted age limits are 4.0, 2.5 and 2.5 Gyr, corresponding to Methods 1, 3, and 5, respectively. The figures show the corresponding gradient (dex kpc^{-1}) and the correlation coefficient in each case.

5. CONCLUSIONS

Based on the results above, the main conclusions of this paper are:

(i) The younger groups have similar or slightly higher oxygen abundances compared with the older groups, especially from the data of Table 2, where the differences may reach about 0.3 dex, higher than the average uncertainties. This can be explained by our current ideas on galactic chemical evolution, since the the observed differences are consistent with the dispersion in the age-metallicity relation, as discussed in the previous section.

(ii) The gradients of both groups are similar within the uncertainties, so that the radial gradient has not

changed appreciably during the lifetimes of the objects considered in this paper, which extend to about 5 Gyr, approximately. Therefore, the PN gradient is not expected to be very different from the gradient observed in HII regions and cepheid variables, which seems to be supported by recent observational data on these objects (cf. Cescutti et al. 2007; Fu et al. 2009; Pedicelli et al. 2009). For example, model results by Cescutti et al. (2007) indicate an O/H gradient of about -0.035 dex kpc^{-1} for the galactocentric range considered here, which is similar to the compiled Cepheid data and also to the present results, as can be seen for instance in Table 1. Similar results for Cepheids and HII regions are also compiled by Fu et al. (2009) and Colavitti et al. (2009). The last reference in particular presents some recent HII data displaying a distribution very similar to the Cepheid data. Also, Pedicelli et al. (2009) present a detailed compilation of Fe abundances in Cepheids with an average slope of -0.05 dex kpc^{-1}. From our own recent work on the oxygen to iron relation in the galactic disk (Maciel, Costa, & Rodrigues 2013), we conclude that the oxygen gradient is approximately 20% smaller than the iron gradient, so that these results are also in agreement with our present results, within the uncertainties.

Our main conclusion on the abundance gradients is in agreement with some recent work by Gibson et al. (2013) and Pilkington et al. (2012), where it is shown on the basis of different sets of observational data and theoretical models that the oxygen gradient apparently has remained approximately constant in the local universe, so that the magnitude of the gradients flattens out for redshift values close to zero.

It would be interesting to extend the present investigation to other elements observed in planetary nebulae, such as Ne, Ar, and S. In fact, some preliminary results, involving a more restricted sample of nebulae for which a morphological classification is possible, support the present results, in the sense that no important differences are observed in the gradients of these elements for younger and older objects. However, these results must still be viewed with caution, as the samples are small and problems such as the "sulphur anomaly" (cf. Henry et al. 2004) are still to be clarified.

It should be stressed that our goal in this paper is to investigate any *temporal variations* of the gradient, and not to determine the actual magnitude of the oxygen gradient. In fact, from the results shown in Tables 1–4, it is apparent that the magnitude of the O/H gradient depends on the adopted sample, especially considering that most PN samples are relatively small. However, it may be concluded that the oxygen gradient is probably in the range $d(\mathrm{O/H})/dR \simeq -0.03$ to -0.07 dex kpc^{-1}, and our suggested average value is $d(\mathrm{O/H})/dR \simeq -0.05$ dex kpc^{-1}, which is essentially the gradient derived from the highly homogeneous sample D, as can be seen from Tables 3 and 4.

REFERENCES

Andreuzzi, G., Bragaglia, A., Tosi, M., & Marconi, G. 2011, MNRAS, 412, 1265

Andrievsky, S. M., Lépine, J. R. D., Korotin, S. A., Luck, R. E., Kovtyukh, V. V., & Maciel, W. J. 2013, MNRAS, 428, 3252

Bahcall, J. N., & Piran, T. 1983, ApJ, 267, L77

Bensby, T., Feltzing, S., & Lundström, I. 2004, A&A, 421, 969

Cahn, J. H., Kaler, J. B., & Stanghellini, L. 1992, A&AS, 94, 399 (CKS)

Cazetta, J. O., & Maciel, W. J. 2000, RevMexAA, 36, 3

Cescutti, G., Matteucci, F., François, P., & Chiappini, C. 2007, A&A, 462, 943

Chiappini, C., Matteucci, F., & Romano, D. 2001, ApJ, 554, 1044

Colavitti, E., Cescutti, G., Matteucci, F., & Murante, G. 2009, A&A, 496, 429

Costa, R. D. D., Uchida, M. M. M., & Maciel, W. J. 2004, A&A, 423, 199

Dias, W. S., Alessi, B. S., Moitinho, A., & Lépine, J. R. D. 2002, A&A, 389, 871

Durand, S., Acker, A., & Zijlstra, A. 1998, A&S, 132, 13

Edvardsson, B., Andersen, J., Gustafsson, B., Lambert, D. L., Nissen, P. E., & Tomkin, J. 1993, A&A, 275, 101

Feltzing, S., Holmberg, J., & Hurley, J. R. 2001, A&A 377, 911

Fu, J., Hou, J. L., Yin, J., & Chang, R. X. 2009, ApJ, 696, 668

Gibson, B. K., Pilkington, K., Bailin, J., Brook C. B., & Stinson, G. S. 2013, XII International Symposium on Nuclei in the Cosmos, Proc. of Science, `http://pos.sissa.it/archive/conferences/146/190/NIC%20XII_190.pdf`

Henry, R. B. C., Kwitter, K. B., & Balick, B. 2004, AJ, 127, 2284

Henry, R. B. C., Kwitter, K. B., Jaskot, A. E., Balick, B., Morrison, M. A., & Milingo, J. 2010, ApJ, 724, 748

Henry, R. B. C., & Worthey, G. 1999, PASP, 111, 919

Holmberg, J., Nordström, B., & Andersen, J. 2007, A&A, 475, 519

_____. 2009, A&A, 501, 941

Hou, J. L., Prantzos, N., & Boissier, S. 2000, A&A, 362, 921

Maciel, W. J., & Costa, R. D. D. 2010, in IAU Symp. 265, ed. K. Cunha, M. Spite, & B. Barbuy (Cambridge: Cambridge Univ. Press), 317

Maciel, W. J., Costa, R. D. D., & Idiart, T. E. P. 2010, A&A, 512, A19
Maciel, W. J., Costa, R. D. D., & Rodrigues, T. S. 2013, ESO Workshop, The Deaths of Stars and the Lives of Galaxies, http://www.eso.org/sci/meetings/2013/DSLG/Presentations/S_I-Maciel.pdf
Maciel, W. J., Costa, R. D. D., & Uchida, M. M. M. 2003, A&A, 397, 667
Maciel, W. J., Lago, L. G., & Costa, R. D. D. 2005, A&A, 433, 127
Maciel, W. J., Rodrigues, T. S., & Costa, R. D. D. 2011, RevMexAA, 47, 401
_____. 2012, in IAU Symp. 283, ed. A. Manchado, L. Stanghellini, & D. Schönberner (Cambridge: Cambridge Univ. Press), 424
Marsakov, V. A., Koval, V. V., Borkova, T. V., & Shapovalov, M. V. 2011, Astron. Rep., 55, 667
Milingo, J. B., Kwitter, K. B., Henry, R. B. C., & Souza, S. P. 2010, ApJ, 711, 619
Nordström, B., et al. 2004, A&A, 418, 989
Pedicelli, S., et al. 2009, A&A, 504, 81
Peimbert, M., 1978, in IAU Symp. 76, ed. Y. Terzian (Dordrecht: Reidel), 215
Pilkington, K., et al. 2012, A&A, 540, A56
Quireza, C., Rocha-Pinto, H. J., & Maciel, W. J. 2007, A&A, 475, 217
Rocha-Pinto, H. J., Maciel, W. J., Scalo, J., & Flynn, C. 2000, A&A, 358, 850
Rocha-Pinto, H. J., Rangel, R. H. O., Porto de Mello, G. F., Bragança, G. A., & Maciel, W. J. 2006, A&A, 453, L9
Soderblom, D. R. 2009, in IAU Symp. 258, ed. E. Mamajek, D. R. Soderblom, & R. Wyse (Cambridge: Cambridge Univ. Press), 1
_____. 2010, ARA&A, 48, 581
Stanghellini, L., Shaw, R. A., & Villaver, E. 2008, ApJ, 689, 194 (SSV)
Stasińska, G. 2004, Cosmochemistry: The Melting Pot of the Elements, ed. C. Esteban, R. J. Garca López, A. Herrero, & F. Sánchez (Cambridge: Cambridge Univ. Press), 115

W. J. Maciel, and R. D. D. Costa: Instituto de Astronomia, Geofísica e Ciências Atmosféricas, Universidade de São Paulo, Rua do Matão 1226, CEP 05508-090, São Paulo SP, Brazil (maciel, roberto@astro.iag.usp.br).